Tellus (2006), 58B, 148–161
Printed in Singapore. All rights reserved

TELLUS

Temporal and spatial variations of oceanic pCO_2 and air–sea CO_2 flux in the Greenland Sea and the Barents Sea

By SHIN-ICHIRO NAKAOKA[1]*, SHUJI AOKI[1], TAKAKIYO NAKAZAWA[1], GEN HASHIDA[2], SHINJI MORIMOTO[2], TAKASHI YAMANOUCHI[2] and HISAYUKI YOSHIKAWA-INOUE[3], [1]*Center for Atmospheric and Oceanic Studies, Graduate School of Science, Tohoku University, Sendai 980–8578, Japan;* [2]*National Institute of Polar Research, Tokyo 173–8515, Japan;* [3]*Laboratory of Marine and Atmospheric Geochemistry, Graduate School of Environmental Earth Science, Hokkaido University, Sapporo 060–0808, Japan*

(Manuscript received 11 April 2005; in final form 7 November 2005)

ABSTRACT

In order to elucidate the seasonal and interannual variations of oceanic CO_2 uptake in the Greenland Sea and the Barents Sea, the partial pressure of CO_2 in the surface ocean (pCO_2^{sea}) was measured in all seasons between 1992 and 2001. We derived monthly varying relationships between pCO_2^{sea} and sea surface temperature (SST) and combined them with the SST data from the NCEP/NCAR reanalysis to determine pCO_2^{sea} and air–sea CO_2 flux in these seas. The pCO_2^{sea} values were normalized to the year 1995 by assuming that pCO_2^{sea} increased at the same growth rate (1.5 μatm yr^{-1}) of the pCO_2 in the air (pCO_2^{air}) between 1992 and 2001. In 1995, the annual net air–sea CO_2 fluxes were evaluated to be 52 ± 20 gC m^{-2} yr^{-1} in the Greenland Sea and 46 ± 18 gC m^{-2} yr^{-1} in the Barents Sea. The CO_2 flux into the ocean reached its maximum in winter and minimum in summer. The wind speed and ΔpCO_2 ($= pCO_2^{air} - pCO_2^{sea}$) exerted a greater influence on the seasonal variation than the sea ice coverage. The annual CO_2 uptake examined in this study (70°–80°N, 20°W–40°E) was estimated to be 0.050 ± 0.020 GtCyr^{-1} in 1995. The interannual variation in the annual CO_2 uptake was found to be positively correlated with the North Atlantic Oscillation Index (NAOI) via wind strength but negatively correlated with ΔpCO_2 and the sea ice coverage. The present results indicate that the variability in wind speed and sea ice coverage play a major role, while that in ΔpCO_2 plays a minor role, in determining the interannual variation of CO_2 uptake in this area.

1. Introduction

The ocean is a major carbon reservoir on the Earth's surface and absorbs a certain amount of anthropogenic CO_2 emitted into the atmosphere. The oceanic CO_2 uptake has been estimated (Keeling and Shertz, 1992; Francey et al., 1995; Keeling et al., 1995; Rayner et al., 1999; Le Quéré et al., 2003), but there are still large uncertainties in their estimates. For example, Prentice et al. (2001) reported an oceanic CO_2 uptake of 1.9 GtC yr^{-1} for the 1990s with an uncertainty of 0.7 GtC yr^{-1} based on an atmospheric O_2/N_2 observation.

It is considered that the vertical transport of carbon from the surface to the deep layer of the ocean plays a key role for the carbon uptake by the ocean. Once carbon is transported from the surface to the abyssal depths of the ocean, either by physical or biological processes, it can be effectively sequestered away from the atmosphere over 1000 years (Broecker and Peng, 1982). In this context, high latitude oceans, such as the Greenland Sea, are thought to be an important sink for atmospheric CO_2 (Anderson, 1995; Noji et al., 2000). In the central Greenland Sea gyre, the Greenland Sea Deep Water, a source water that ventilates the North Atlantic Deep Water, is formed (Aagaard et al., 1985).

A positive or negative difference in the partial pressure (or fugacity) of CO_2 between the air and the sea (ΔpCO_2 or ΔfCO_2) determines the direction of the CO_2 flux across the air–sea interface. Compared with the partial CO_2 pressure in the air (pCO_2^{air}), the partial pressure in surface seawater (pCO_2^{sea}) varies considerably, both spatially and temporarily. For example, Takahashi et al. (2002) showed that the pCO_2^{sea} ranged from 155 μatm in the northern Greenland Sea (80°N, 7.5°E) in July to 529 μatm in the Arabic Sea (16°N, 62.5°E) in July, a significantly large

*Corresponding author.
e-mail: syn@caos-a.geophys.tohoku.ac.jp

value when compared with that of pCO_2^{air} (25 μatm). In the Greenland Sea gyre, Hood et al. (1999) evaluated an annual average ΔfCO_2 of 71 μatm based on a 6-month measurement by CARIOCA drift buoys. They estimated an oceanic CO_2 uptake of 2.4 to 4.2 $\times$ 10^{-3} GtC yr^{-1} for the Greenland Sea gyre (74°–76°N, 10°W–5°E; 0.15 $\times$ 10^6 km^2) in the period from August 1996 to July 1997. Skjelvan et al. (1999) derived a CO_2 uptake of 1.2 $\pm$ 0.15 $\times$ 10^{-1} GtC yr^{-1} for the Greenland Sea (0.81 $\times$ 10^6 km^2) and the Norwegian Sea (1.39 $\times$ 10^6 km^2) based on their observed data from the regions of 74.5°–75.5°N and 5°W–3°E (25.6 $\times$ 10^3 km^2) and 64.5°–70.5°N and 7°W–5°E (33.8 $\times$ 10^3 km^2) during the 1996–1997 period. By analyzing the fCO_2^{sea} values measured during nine cruises between 1982 and 1998, Olsen et al. (2003) reported a CO_2 uptake of 8.2 $\times$ 10^{-2} GtC yr^{-1} for the northern North Atlantic (45°–80°N) in the wintertime (October to March), with an interannual variability of about $\pm$ 7% due mostly to changes in the wind speed and fCO_2^{air}.

The formation of intermediate/deep water also occurs in the Barents Sea (Kaltin et al., 2002). High density water is formed on the shelf of the Barents Sea by surface cooling and brine rejection due to sea ice formation and then penetrates to the intermediate/deep layers in the Arctic Ocean. Schlosser et al. (1990) pointed out that atmospheric CO_2 absorbed by the Barents Sea would be stored in the Arctic Ocean for more than 100 years. Based on measurements of the total dissolved inorganic carbon, total alkalinity, temperature, salinity and nitrate in the water column, Kaltin et al. (2002) calculated the oceanic CO_2 uptake to be 29 $\pm$ 11 gC m^{-2} for 3 months starting from the late winter of 1999.

In order to discuss the variations in oceanic CO_2 uptake along with factors controlling the air–sea CO_2 flux (ΔpCO_2, wind speed and the sea ice area) in the Greenland Sea and the Barents Sea in more detail, it is important to obtain extensive sets of the pCO_2^{sea} data for those seas.

In this study, we acquired the pCO_2^{sea} data in the Greenland Sea and the Barents Sea for the 1992–2001 period and then calculated the air–sea CO_2 fluxes from those data and atmospheric CO_2 measurements from a nearby site at Ny-Ålesund (79°N, 12°E). We then examined the seasonal/interannual variations of the oceanic CO_2 uptake in terms of the ΔpCO_2, SST, wind and sea ice coverage to show how these factors affect the air–sea CO_2 flux in the Greenland Sea and the Barents Sea.

2. Sampling and analytical methods

2.1. Measurements of pCO_2^{sea}

Comprehensive measurements of the pCO_2^{sea} and its relevant factors were made during nine cruises in the eastern Greenland Sea and the western Barents Sea from August 1992 to April 2001, as summarized in Table 1. Hydrographic stations for the pCO_2^{sea} measurements, major current system (Furevik, 2001) and minimum/maximum sea ice area as determined by the NCEP/NCAR reanalysis data (Kalnay et al., 1996) are depicted in Fig. 1. There are two branches of the warm Norwegian Atlantic Current that flow northward off the Norwegian coast; one is the West Spitsbergen Current, and the other is the branch that enters the Barents Sea (Furevik, 2001; Kaltin et al., 2002). The cold Eastern Greenland Current flows southward along Greenland.

The pCO_2^{sea} values were obtained using a discrete flask sampling with subsequent laboratory analysis. The sampling system for air equilibrated with seawater consisted of a shower-head type equilibrator, a diaphragm pump, a chemical desiccant column ($Mg(ClO_4)_2$), a four-way valve and a stainless flask (1 L) with two stopcocks at both ends (Watai et al., 1998). The equilibrator was vented to the atmosphere so that air samples were collected at ambient pressures. All the flasks were evacuated at 1.3 $\times$ 10^{-5} Pa at 120 °C for 24 hours in our laboratory before shipping, and each flask was thoroughly flushed by uncontaminated air aboard ship before sampling. After connecting the flask to the sampling system, the air was circulated at a flow rate of 0.5 L min^{-1} for 15 minutes to ensure equilibrium in CO_2 between seawater and air (Watai et al., 1998), and then collected in the flask.

From August 1992 to January 1999, seawater was taken 3–5 m below the surface using a submersible pump (>100 L min^{-1}), and part of it (12 L min^{-1}) was diverted into the equilibrator. It was found that the temperature of seawater in the equilibrator agreed well with SST to within $\pm$ 0.1 °C. During November 1999 and April 2001, uncontaminated seawater was taken from the

Table 1. Summary of cruises in the Greenland Sea and the Barents Sea for the 1992–2001 period

Year	Month	Cruise name	Vessel name	Observed territory	Sampling method
1992	Aug.	-	LANCE	75°–79°N 11°W–9°E	Anchor
1993	Aug.	-	LANCE	74°–79°N 13°W–9°E	Anchor
1994	April–May	-	POLAR SHIP	70°–75°N 18°W–10°W	Anchor
1995	June	ICE BAR	LANCE	74°–78°N 19°E–35°E	Anchor
1996	July–Aug.	ICE BAR	LANCE	74°–81°N 17°E–35°E	Anchor
1999	Jan.–Feb.	- / VEINS	IAN PETROV / LANCE	70°–80°N 0°–30°E	Anchor
1999	Nov.	VIENS	LANCE	71°–80°N 11°E–20°E	Underway
2000	October	-	LANCE	71°–78°N 13°E–19°E	Underway
2001	April	CONVECTION	LANCE	71°–77°N 11°W–19°E	Underway

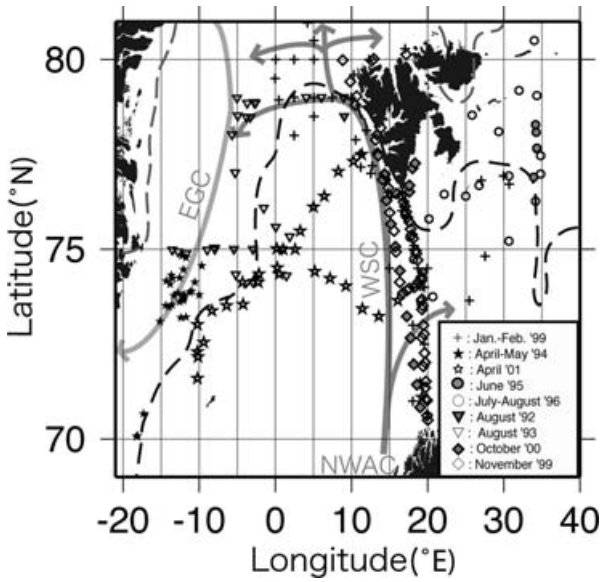

Fig. 1. Geographical locations where pCO_2^{sea} measurements were made from 1992 through 2001. The atmospheric CO_2 data used to calculate pCO_2^{air} in this study were taken at Ny-Ålesund in the Svarbard Islands (79°N, 12°E). The dashed grey line shows the boundary of the climatological sea ice area in August, and the dashed black line shows the climatological sea ice area in January. The arrows represent the major currents in the Greenland Sea and the Barents Sea (Furevik , 2001), including the Norwegian Atlantic Current (NWAC), West Spitsbergen Current (WSC) and East Greenland Current (EGC).

sea-chest of the vessel, and it was observed that the temperature of seawater in the equilibrator was higher than SST by 0.55 °C in November 1999 and 0.82 °C in April 2001. In October 2000, we did not measure the seawater temperature rise in the equilibrator. Therefore, the average of the two values for November 1999 and April 2001 (0.68 °C) was taken to be the rise in seawater temperature from the inlet to the equilibrator. The uncertainty in the temperature rise was considered to be 0.14 °C in October 2000, but this does not affect the results of the present study (see Section 3.3).

All the flasks filled with air samples were sent to our laboratory, and their CO_2 concentrations were determined against our air-based CO_2 standard gases with a precision of ± 0.5 ppmv within 3 months of sampling using a gas-chromatograph equipped with a flamed ionization detector and a converter of CO_2 to CH_4 (Watai et al., 1998). The CO_2 concentrations of our standard gases are traceable to the WMO standards (Tanaka et al., 1987; http://gaw.kishou.go.jp/wcc/co2/co2comparison). We also confirmed that the CO_2 concentrations of air samples stored in our flasks were stable to within ± 0.1 ppmv for 3 months (Nakazawa et al., 1997).

The values of the pCO_2^{sea}, as well as those of the pCO_2^{air}, were calculated by the equation

$$pCO_2 = xCO_2 \times (P - p(H_2O)). \quad (1)$$

Here, xCO_2 is the measured CO_2 concentration of dry air equilibrated with seawater or that of ambient dry air at Ny-Ålesund, P is the barometric pressure and $p(H_2O)$ is the saturated vapour pressure. As mentioned above, the temperature of seawater rose between the inlet and the equilibrator during three cruises after 1999. This effect on the measured values of pCO_2 was corrected using the iso-chemical temperature dependence of pCO_2 given by Takahashi et al. (1993),

$$\frac{\delta \ln(pCO_2)}{\delta T} = 4.23\ (\%\quad {}^{\circ}C^{-1}). \quad (2)$$

The pCO_2^{sea} data used in this work will be sent to WMO WDCGG (Tokyo, Japan) and CDIAC (Oak Ridge, USA) in the near future.

2.2. Calculation of the air–sea CO_2 flux

The CO_2 flux (f) between the air and the sea is conventionally given by the product of the gas transfer velocity K_{CO2} as a function of wind speed (Wanninkhof, 1992; Wanninkhof and McGills, 1999), the solubility of $CO_2\beta$ (Weiss, 1974) and the partial pressure difference ΔpCO_2;

$$f = K_{CO_2} \cdot \beta \cdot \left(pCO_2^{air} - pCO_2^{sea}\right)$$
$$= K_{CO_2} \cdot \beta \cdot \Delta pCO_2 = E \cdot \Delta pCO_2. \quad (3)$$

Here, E represents the gas transfer coefficient, which is usually assumed to be independent of SST, since K_{CO2} and β counteract their temperature dependence on each other (Tans et al., 1990). We then determined the pCO_2^{sea}-SST relationships after normalizing pCO_2^{sea} to the year 1995 to interpolate/extrapolate to a larger region. To calculate the monthly averaged CO_2 fluxes for the 1992–2001 period, we used the NCEP/NCAR reanalysis data (Kalnay et al., 1996) for the SST, wind speed, atmospheric pressure and sea ice distribution. Since the NCEP/NCAR reanalysis data are prepared for each grid of 1.875° by 1.904°, the air–sea CO_2 fluxes were also obtained on the same spatial resolution. Therefore, the total CO_2 flux in the whole area is presented by the equation

$$F = \sum_{i=0}^{n} (E_i \cdot \Delta pCO_{2,i} \cdot S_i). \quad (4)$$

Here, i represents the grid number, and S shows the sea area. In this calculation, we assumed that the CO_2 exchange across the air–sea interface is thoroughly prevented by the sea ice.

2.3. Uncertainties

We evaluated the uncertainties in the present estimates of the CO_2 flux to be 39% by accounting for uncertainties associated with ΔpCO_2 derived using the pCO_2^{sea}-SST relationship and the measured values of pCO_2^{air}, wind speed and SST. We estimated 25% as the uncertainty of ΔpCO_2. For the NCEP/NCAR reanalyzed wind speed and SST, we employed the uncertainties

reported by Smith et al. (2001) for the North Atlantic Ocean (9% for the wind speed and 16% for SST).

3. Results and discussion

3.1. Long-term trend of pCO_2^{sea} and pCO_2^{air}

The pCO_2^{sea} values obtained in the western Greenland Sea in April 1994 and in the same month in 2001 were compared to determine the long-term trend. The comparison indicated a pCO_2^{sea} increase of 28 ± 21 μatm, on average, during that period. However, further detailed discussion of the long-term trend is beyond the scope of this paper because the spatial variability is too large and time series data are not available for that region.

Recent studies have revealed a secular increase of pCO_2^{sea} in the subtropics (Gruber et al., 2002; Keeling et al., 2004; Midorikawa et al., 2005) and even in the high latitudes, such as the Southern Ocean (Inoue and Ishii, 2005) and northern North Atlantic, where deep convection occurs in winter. In the Barents Sea, Omar et al. (2003) compared the fCO_2^{sea} data taken in 1967 and in 2000–2001. They found that fCO_2^{sea} has increased at a rate similar to the atmospheric CO_2 increase over the past 33 years. By inspecting observational data from the northern North Atlantic, Olsen et al. (2003) found that the pCO_2^{sea} has increased at a rate larger than that of the pCO_2^{air}. Furthermore, Lefèvre et al. (2004) reported that the pCO_2^{sea} has increased at a rate of 1.8 μatm yr^{-1} in recent decades, which is slightly higher than that of the pCO_2^{air}, in the North Atlantic (50°–70°N, 80°–10°W).

In this study, we simply assumed that the pCO_2^{sea} has increased at a rate equal to that observed for pCO_2^{air} (Olsen et al., 2003; Omar et al., 2003). The pCO_2^{air} values were derived from the atmospheric CO_2 concentration data at Ny-Ålesund (Morimoto et al., 2001), which show an average increase rate of 1.5 ppmv yr^{-1} for the 1992–2001 period. By assuming the increase rate to be 1.5 μatm yr^{-1} for pCO_2^{sea}, we normalized all the observed data of pCO_2^{sea} to the year 1995 ($pCO_{2,95}^{sea}$) to evaluate the seasonal variation in the air–sea CO_2 flux.

3.2. pCO_2^{sea}-SST relationships for the Greenland Sea and the Barents Sea

The data of pCO_2^{sea} are unevenly distributed in space and time; thus, it is necessary to interpolate/extrapolate the observed pCO_2^{sea} values to evaluate the annual CO_2 uptake in the Greenland Sea and the Barents Sea. It is known that variations in pCO_2^{sea} are mainly due to changes in temperature, mixing of the upper ocean and marine biological activities (Broecker and Peng, 1982). The pCO_2^{sea} variations are often apparently related to SST (e.g. Tans et al., 1990; Inoue et al., 1995; Cosca et al., 2003). Seasonal variation in the relative contribution of those processes influencing pCO_2^{sea} leads to a different temperature dependence of pCO_2^{sea}. Therefore, we determined the apparent relationships between the pCO_2^{sea} and SST for each month and combined them with the data set of SST that is available throughout these seas.

Figure 2 shows the relationships between the $pCO_{2,95}^{sea}$ and SST for the Greenland Sea and the Barents Sea. The temperature dependence of $pCO_{2,95}^{sea}$ is noticeably different for different seasons.

The $pCO_{2,95}^{sea}$ increases with increasing SST, except for May and June. The temperature dependence of $pCO_{2,95}^{sea}$ varied from 1 to 3% °C^{-1} from August to April. These temperature dependences deviate from that of the solubility (eq. (2)), which suggests the effect of the mixing of the upper ocean and biological activities against SST change. In May, when SST was lower than 1 °C, we found a negative correlation between $pCO_{2,95}^{sea}$ and SST. This relationship may be closely related to the biological CO_2 uptake, which starts in the western area of the Greenland Sea at this time of the year (Skjelvan et al., 1999; Anderson et al., 2000). In June, a higher $pCO_{2,95}^{sea}$ (>250 μatm) was observed when SST > 2 °C and < –1 °C, and a lower $pCO_{2,95}^{sea}$ (<200 μatm) was observed when SST was about 1 °C. A large temperature dependence of $pCO_{2,95}^{sea}$ was noted in July (6% °C^{-1}). This might be caused by the CO_2 drawdown close to the sea ice in the western Barents Sea (Fig. 1). Such a complicated $pCO_{2,95}^{sea}$-SST relationship also indicates that processes other than solubility, possibly biological activities (spring bloom), predominantly control the variation in $pCO_{2,95}^{sea}$. Therefore, we tried to derive the $pCO_{2,95}^{sea}$ values during the spring bloom using SST and chlorophyll-a data. However, $pCO_{2,95}^{sea}$ could not be approximated by these two parameters alone, as pointed out in the equatorial Pacific by Dandonneau (1995) earlier. To document the pCO_2^{sea} distribution during the spring bloom, it is necessary to use variables that are directly related to the photosynthesis/respiration of phytoplankton, such as nitrate and phosphate (Wanninkhof et al., 1996).

3.3. ΔpCO_2 maps for the Greenland Sea and the Barents Sea

In order to draw monthly maps of $pCO_{2,95}^{sea}$ for the Greenland Sea and the Barents Sea, we used seasonally different $pCO_{2,95}^{sea}$-SST relationships obtained by fitting the data given in Fig. 2 with

$$pCO_{2,95}^{sea}(t) = a(t) \times SST + b(t), \quad (5)$$

where $a(t)$ is the slope and $b(t)$ the intercept at a given time (month) t. In this procedure, since the pCO_2^{sea} values observed at SST higher than 2 °C in June are fairly close to those for July, we included those data to derive the $pCO_{2,95}^{sea}$-SST relationship for July. We also assumed that the negative relationship found in May is valid at SST lower than 0.55 °C in June, and the positive relationship at SST higher than 0.55 °C in June/July is applicable to the same SST range in May. The temperature of 0.55 °C is the intersecting point of the two $pCO_{2,95}^{sea}$-SST regression lines shown in Fig. 2(b). For January and February, the same positive

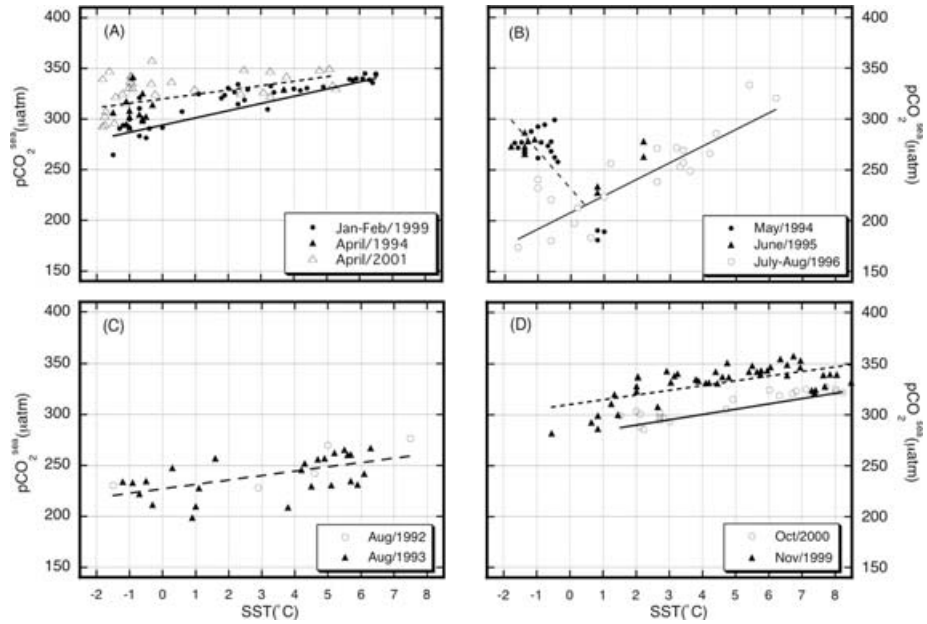

Fig. 2. Relationships between pCO_2^{sea} and SST for the Greenland Sea and the Barents Sea for the periods of January to April (A), May to early August (B), late August (C) and October to November (D). All the pCO_2^{sea} values plotted were normalized to the year 1995, assuming that they have increased secularly at the same rate as pCO_2^{air} (1.5 μatm yr^{-1}). The solid and dashed lines show the values obtained by applying a least-squares fit to the data.

Table 2. Coefficients of the linear function (eq. (4) in the text) expressing the pCO_2^{sea}-SST relationships for the respective months derived on the basis of the pCO_2^{sea} data taken in the Greenland Sea and the Barents Sea for the 1992–2001 period. a, b, N, σ, r and ci represent the slope (μatm °C^{-1}) and intercept (μatm) of the linear function determined by a least-squares fit, the volume of data used, the standard deviation (μatm), the correlation coefficient of the fit and the 95% confidence interval, respectively

Month	a	b	N	σ	r	ci
1	7.10	294.02	22	10	0.88	0.73–0.95
2	7.10	294.02	18	10	0.88	0.70–0.95
3	5.90	305.37	-		-	-
4	4.35	320.05	40	14	0.60	0.35–0.77
5–6 (SST<0.55 °C)	−33.99	235.85	20	11	−0.59	−0.82 to −0.20
5–6 (SST>0.55 °C)	16.37	208.08	7	28	0.82	0.18–0.97
7	16.37	208.08	14	17	0.94	0.82–0.98
8	8.11	222.09	27	15	0.64	0.34–0.82
9	4.77	250.55	-		-	-
10	5.23	279.45	21	5	0.92	0.81–0.97
11	4.67	310.10	48	13	0.63	0.42–0.78
12	5.99	301.39	-		-	-

$pCO_{2,95}^{sea}$-SST relationship was used, considering active deep convection and low marine biological activities in this period of the year. Furthermore, under the assumption that the $pCO_{2,95}^{sea}$-SST relationship varies smoothly with time, the slope and the intercept for March, September and December with no observational data were deduced by interpolating linearly the results of contiguous months. The respective parameters obtained by fitting to eq. (5) are summarized in Table 2. As shown in Fig. 3, the values of $pCO_{2,95}^{sea}$ calculated using eq. (5) with the best-fit parameters agreed well with the observed $pCO_{2,95}^{sea}$ values with a standard deviation of $\pm$ 14 μatm for the differences between the observed and calculated values.

To see the seasonal cycles of $pCO_{2,95}^{sea}$ calculated by eq. (5) and to examine whether they could reconstruct the actual features throughout the year, we compared the $pCO_{2,95}^{sea}$ values by eq. (5) and observational data taken in the present with those of

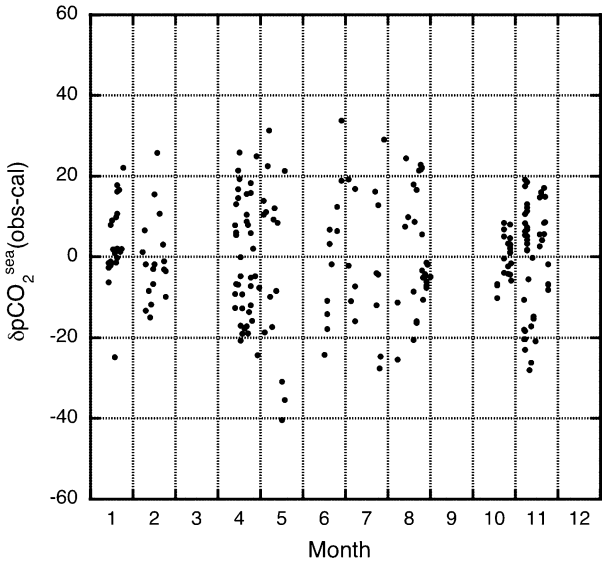

Fig. 3. Differences between the observed and calculated pCO_2^{sea} values for the Greenland Sea and the Barents Sea. The calculated values were obtained from the empirically derived pCO_2^{sea}-SST relationships and the SST data (*cf*. text).

earlier studies (Weiss et al., 1992; Hood et al., 1999; Anderson et al., 2000; Takahashi et al., 2002; Olsen et al., 2003; Omar et al., 2003) for two sites at 75°N, 0° in the central Greenland Sea and at 74°N, 17.5°E in the western Barents Sea (Fig. 4). The $pCO_{2,95}^{sea}$ values calculated in this study are 15–30 μatm higher than those observed by Weiss et al. (1992) in the Greenland Sea in July 1981 and in March 1982. However, if the pCO_2^{sea} increased at the same rate as pCO_2^{air} from 1981 to 1995, the calculated pCO_2^{sea} values agree well with the observed values within a range of –9 to 6 μatm. This means that our assumption about the annual increase of pCO_2^{sea} is generally reasonable.

The calculated $pCO_{2,95}^{sea}$ in the central Greenland Sea (Fig. 4(a)) shows a seasonal variation of about 95 μatm, with two maxima, one in April and another in November, and a minimum in June. Anderson et al. (2000) reported a seasonal variation of fCO_2^{sea} with a maximum in November and a minimum in August. Furthermore, we compared our $pCO_{2,95}^{sea}$ values with those of Olsen et al. (2003). Their equation gives the pCO_2^{sea} values in the year 1995 and is applicable to the period from October to March. The values of pCO_2^{sea} calculated by Olsen et al. (2003) for the October–March period agree well with our results within a range of 3 to 14 μatm, except for October. In October, a large difference of 32 μatm was found between the pCO_2^{sea} values of this study and those observed by Olsen et al. (2003). The fCO_2^{sea} values given by Hood et al. (1999) and Anderson et al. (2000) are generally higher than our calculated values. On the other hand, the average values of pCO_2^{sea} obtained by Takahashi et al. (2002) for two sites (76°N, 2.5°W and 76°N, 2.5°E) are 15–25 μatm lower than those of our results, showing a seasonal

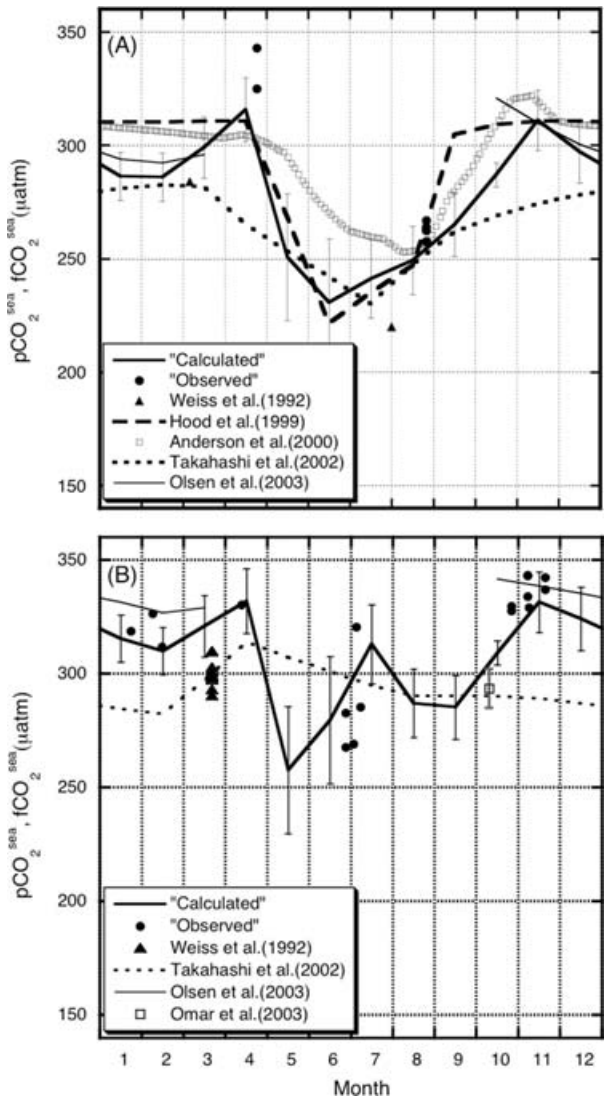

Fig. 4. Seasonal variations of pCO_2^{sea} in the central Greenland Sea (panel a) and the western Barents Sea (panel b). The thick solid lines in the upper and lower panels show the pCO_2^{sea} values calculated for the respective locations at 75°N and 0° and 74°N and 17.5°E using the empirical pCO_2^{sea}-SST relationships with coefficients given in Table 2. The solid circles represent our observed pCO_2^{sea} values normalized to the year 1995. In panel (a), the solid triangles denote the pCO_2^{sea} observed by Weiss et al. (1992) for 1981 and 1982, the dotted line, the fCO_2^{sea} by Hood et al. (1999), the rectangle, the fCO_2^{sea} by Anderson et al. (2000), the dashed line, the pCO_2^{sea} by Takahashi et al. (2002) and the solid thin line, the fCO_2^{sea} calculated using the fCO_2^{sea}-SST relationships given empirically by Olsen et al. (2003). In panel (b), the solid triangles show the pCO_2^{sea} values observed by Weiss et al. (1992) for 1981 and 1982, the dashed line, the pCO_2^{sea} by Takahashi et al. (2002) and the rectangle, the pCO_2^{sea} derived for an SST of 5.7 °C from the results obtained by Omar et al. (2003) for October.

variation with high values in February/March and low values in July.

As seen in Fig. 4(b), $pCO_{2,95}{}^{sea}$ varied largely on a time scale of a few months in the western edge of the Barents Sea. The $pCO_{2,95}{}^{sea}$ showed a hump in July, which is caused by the large temperature dependence of $pCO_{2,95}{}^{sea}$ in June and July (Table 2). The $pCO_{2,95}{}^{sea}$ values calculated for March also agreed well with those obtained by Weiss et al. (1992), if their $pCO_2{}^{sea}$ values are shifted up by an amount equivalent to the rise in $pCO_2{}^{air}$ over the period in question. Omar et al. (2003) obtained a $pCO_2{}^{sea}$ value for October that was slightly lower than our values, and the results by Olsen et al. (2003) for the October–March period agree well with ours, except for October. In October, a large difference of 32 μatm was also found between the $pCO_{2,95}{}^{sea}$ values and those observed by Olsen et al. (2003). The $pCO_2{}^{sea}$ values by Olsen et al. (2003) deviate largely from ours in the Greenland Sea and the Barents Sea in October, due to the difference in temperature dependence of $pCO_2{}^{sea}$ between both studies.

The average values of $pCO_2{}^{sea}$ given by Takahashi et al. (2002) for two sites (76°N, 17.5°E and 72°N, 17.5°E) show a rapid increase from February to April, with a gradual monotonic decrease thereafter towards the minimum in autumn and winter; the seasonal evolution identified by Takahashi et al. (2002) has a noticeably different temporal behaviour than that in our results.

The $pCO_{2,95}{}^{sea}$ of the western Barents Sea is higher than that of the central Greenland Sea. However, the seasonal variation in the $pCO_{2,95}{}^{sea}$ of the western Barents Sea showed a different pattern from that of the central Greenland Sea (Figs. 4(a) and 4(b)). These variations were caused by the monthly varying temperature dependence of the $pCO_{2,95}{}^{sea}$ and SST distribution. In the western Barents Sea, SST is about 2–3 °C higher than the SST in the central Greenland Sea throughout the year.

The monthly distributions of $pCO_{2,95}{}^{sea}$ for the Greenland Sea and the Barents Sea are presented in Fig. 5. The area of sea ice was at its minimum in August and at its maximum in January (Fig. 1). The warm West Spitsbergen Current and the cold Eastern Greenland Current produce the longitudinal characteristics of a $pCO_{2,95}{}^{sea}$ distribution that is high on the east side and low on the west side, reflecting mainly the temperature dependence of $pCO_{2,95}{}^{sea}$. The current flowing northeastward in the Barents Sea originated from the Norwegian Atlantic Current (Fig. 1) shows relatively high $pCO_{2,95}{}^{sea}$ in comparison with the surrounding areas.

In May and June, $pCO_{2,95}{}^{sea}$ in the western Greenland Sea decreases to levels lower than 250 μatm, depending on SST. In the spring of 1995, Skjelvan et al. (1999) found that the values of $fCO_2{}^{sea}$ measured along 75°N were similar to the winter values in the eastern area of the Greenland Sea and that $fCO_2{}^{sea}$ decreased rapidly from about 320 to 240 μatm at 3°W due to the CO_2 drawdown by biological activities in the western area. However, in the spring of 1997, they also found that the $fCO_2{}^{sea}$ values in the western area were relatively constant (270–300 μatm), probably due to unusually cold temperatures at that time (Chierici, personal communication).

3.4. Seasonal variation of the air–sea CO_2 flux

Based on the monthly distributions of $pCO_{2,95}{}^{sea}$ given in Fig. 5 and $pCO_2{}^{air}$ at Ny-Ålesund, the air–sea CO_2 fluxes in the Greenland Sea and the Barents Sea were calculated for the respective months. The results are shown in Fig. 6. In general, the Greenland Sea and the Barents Sea are sinks for the atmospheric CO_2. The flux is small (<2 mol m^{-2} yr^{-1}) in the eastern Greenland Sea because warm currents with small ΔpCO_2 are flowing in this region (Skjelvan et al., 1999; Olsen et al., 2003). By contrast, larger CO_2 fluxes (>6 mol m^{-2} yr^{-1}) are found in the northwestern area for the period of December to March, which is ascribed to strong winds (7–9 m s^{-1}) as well as to low $pCO_{2,95}{}^{sea}$. In May and June, larger air-to-sea CO_2 fluxes are inferred in the areas where the negative $pCO_{2,95}{}^{sea}$-SST relationship was applied to derive $pCO_{2,95}{}^{sea}$. During the period from July to September, when the wind speed ranges between 3 and 6 m s^{-1}, the CO_2 flux is reduced by 70% compared with the wintertime value, even for the same ΔpCO_2.

The air–sea CO_2 fluxes estimated for the Greenland Sea and the Barents Sea are summarized in Tables 3 and 4, respectively, along with those reported in earlier studies. Our result for the Greenland Sea (52 $\pm$ 20 gC m^{-2} yr^{-1}) agrees well with those of earlier studies. From the calculation of $fCO_2{}^{sea}$ based on measurements of the total dissolved inorganic carbon, total alkalinity, temperature, salinity and phosphorous concentrations in the central Greenland Sea (75°N, 0°) for the 1993–1997 period, Anderson et al. (2000) estimated the average annual CO_2 flux to be 53 $\pm$ 4 gC m^{-2} yr^{-1}. Hood et al. (1999) also reported a CO_2 flux of 55 gC m^{-2} yr^{-1} for the last 2 years of the period, 1996 and 1997. On the other hand, Skjelvan et al. (1999) gave a somewhat larger CO_2 flux of 71 gC m^{-2} yr^{-1} for the 1993–1995 period. For the Barents Sea, we estimated the annual CO_2 flux to be 46 $\pm$ 27 gC m^{-2} yr^{-1}. This value also agrees well with that of 44 $\pm$ 10 gC m^{-2} yr^{-1} derived by Fransson et al. (2001).

However, a more detailed inspection of Tables 3 and 4 indicates noticeable differences in the seasonal behaviour of the CO_2 flux observed in the present and earlier studies. The CO_2 uptake estimated by Skjelvan et al. (1999) for the Greenland Sea in summer and autumn is larger than ours. This difference can be attributed to the wind speed used to calculate the air–sea CO_2 flux. Compared with our values, the ΔpCO_2 values given by Skjelvan et al. (1999) are about 13 μatm higher in summer and 11 μatm lower in autumn. These differences would yield only a 10% difference in the air–sea CO_2 flux under the same wind conditions. On the other hand, the NCEP/NCAR data used in this study give average wind speeds of 5.4 and 8.5 m s^{-1} for summer and autumn, respectively, and Skjelvan et al. (1999) used wind speeds of 7.2 and 11.2 m s^{-1} for the respective seasons in their

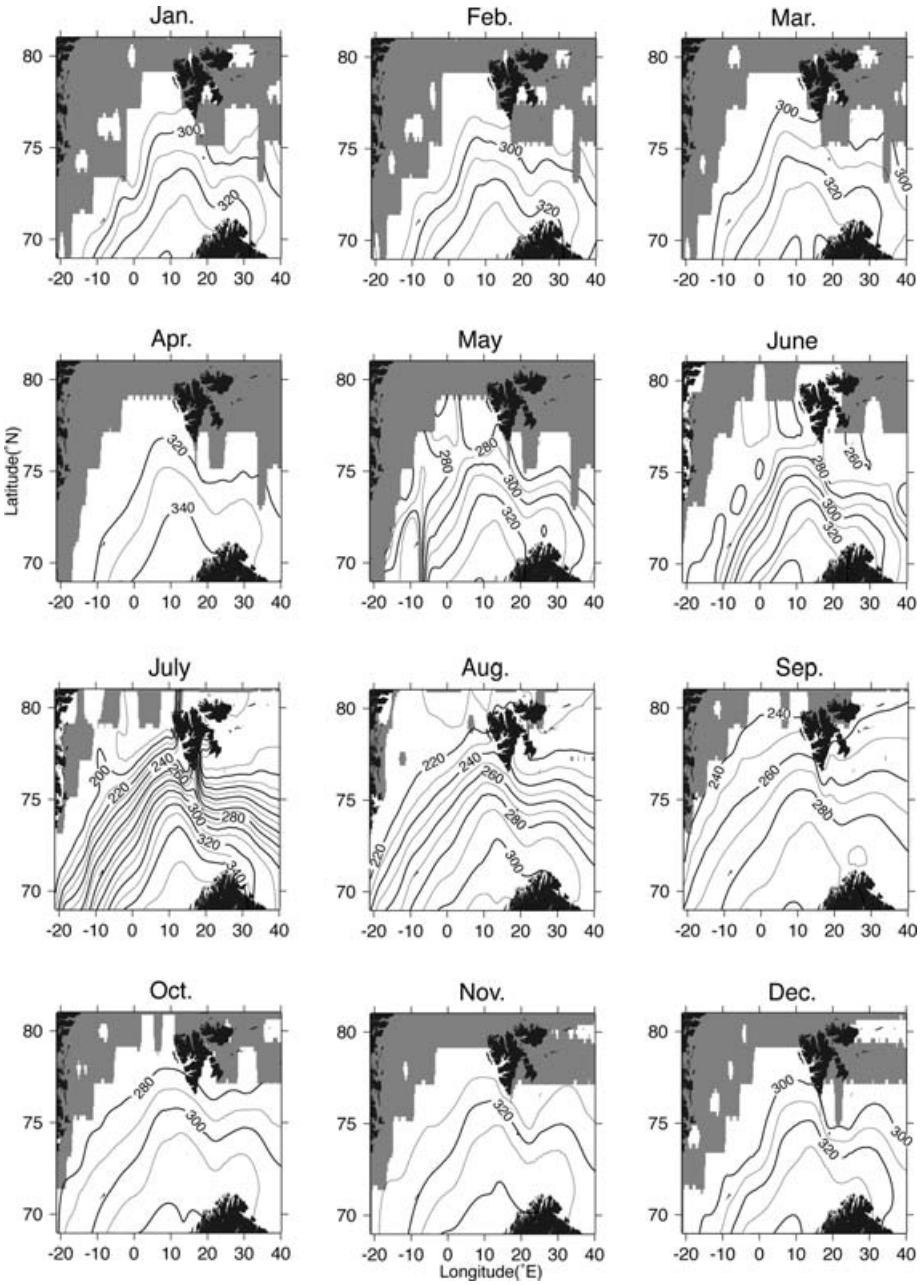

Fig. 5. Distributions of the monthly pCO_2^{sea} values (μatm) calculated for 1995 using the empirical pCO_2^{sea}-SST relationships and the NCEP/NCAR reanalysis SST data. The shaded areas show the sea ice estimated based on the NCEP/NCAR reanalysis data.

analysis. By changing the wind speed in the range covered by both studies, the air–sea CO_2 flux can be altered by a factor of 2. For winter and spring, Skjelvan et al. (1999) used almost the same wind and ΔpCO_2 fields as ours. Therefore, there is a better agreement between the results of both studies for these seasons than for summer and autumn.

The CO_2 fluxes derived by Hood et al. (1999) using the ECMWF wind data agree well with our results within our estimated uncertainties. The oceanic CO_2 uptake estimated by Kaltin et al. (2002) for the Barents Sea depends largely on the C/N ratio of new production. Their estimate of the CO_2 flux, 44 ± 40 gC m^{-2} yr^{-1}, agrees fairly well with the estimate in this study when the C/N ratio is assumed to be 6.6.

It is important to clarify how the seasonal evolution of the CO_2 uptake in the Greenland Sea and the Barents Sea is controlled by various oceanic and atmospheric phenomena. Figure 7 shows the monthly averages of the ΔpCO_2, relative ice cover, wind speed and the CO_2 uptake for the region (70°–80°N,

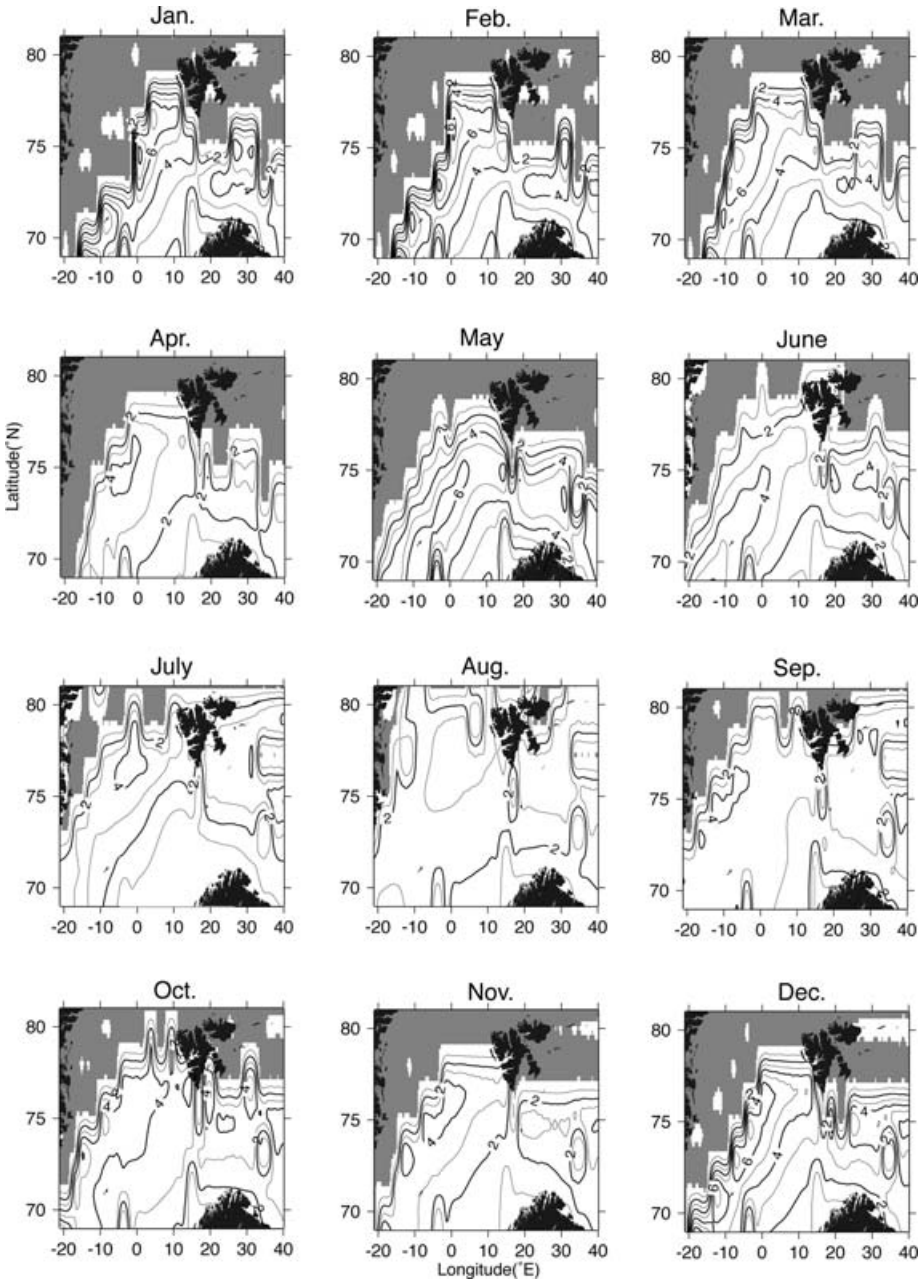

Fig. 6. Distributions of the monthly air–sea CO_2 fluxes (mol m^{-2} yr^{-1}) calculated for 1995 using the gas transfer velocity given by Wanninkohf (1992) and the monthly average wind fields derived from the NCEP/NCAR reanalysis data for the 1992–2001 period. The positive flux values indicate the uptake of atmospheric CO_2 by the ocean, and the shaded areas show sea ice.

20°W–40°E) covered by the Greenland Sea and the Barents Sea. In general, the seasonal variation of ΔpCO_2 is negatively correlated with the wind speed, and, to a lesser extent, with the ice cover. The monthly CO_2 uptake reaches low values (0.034 GtC yr^{-1}) in April and November and high values (0.062 GtC yr^{-1}) in May and September, reflecting different seasonal variations of the variables used in its calculation. In order to quantify how ΔpCO_2, the gas transfer velocity and the relative ice cover affect the CO_2 uptake, we used the equation

$$F_{a.f.}(t) = \overline{E}(t) \cdot \Delta\overline{pCO_2}(t) \cdot S(t), \quad (6)$$

where $F_{a.f.}(t)$ is the total CO_2 uptake in the Greenland Sea and the Barents Sea, $S(t)$ is the ice-free sea area, $\Delta\overline{pCO_2}(t)$ is the spatially averaged value of ΔpCO_2 at month t and $\overline{E}(t)$ is the spatially averaged value of the gas transfer velocity $E(t)$. This equation disregards the covariance term between the transfer

Table 3. Air–sea CO_2 fluxes (gC m^{-2} yr^{-1}) in winter (January to March), spring (April to June), summer (July to September) and autumn (October to December), and annual CO_2 fluxes in the open water areas of the central Greenland Sea

	Winter	Spring	Summer	Autumn	Annual
Hood et al. (1999)	58	64	52	43	55
Skjelvan et al. (1999)	$58 \pm 14_{(1995)}$	$52 \pm 21_{(1995)}$	$77 \pm 26_{(1993)}$	85 ± 16 (1995)	71
Anderson et al. (2000)	-	-	-	-	53 ± 4
Olsen et al. (2003)	$44 \sim 61_{(Feb.)}$	-	-	$35 \sim 53$ (Nov.)	-
This work	72 ± 25	45 ± 21	37 ± 14	54 ± 21	52 ± 20

The uncertainties of Skjelvan et al. (1999) are estimated based on the standard deviations in wind speed and natural variability observed in the fCO_2^{sea} measurements. The uncertainty of Anderson et al. (2000) is due to the variability in the wind field and extent of sea ice from 1993 to 1997.

Table 4. Air–sea CO_2 fluxes (gC m^{-2} yr^{-1}) in winter (January to March), spring (April to June), summer (July to September) and autumn (October to December), and annual CO_2 fluxes in the open water areas of the Barents Sea

	Winter	Spring	Summer	Autumn	Annual
Fransson et al. (2001)	-	-	-	-	44 ± 10
Kaltin et al. (2002)	-	116 ± 44 (C/N=8.75)	-	-	-
	-	44 ± 40 (C/N=6.6)			
This work	63 ± 22	28 ± 13	43 ± 17	49 ± 18	46 ± 18

The uncertainties of Kaltin et al. (2002) include the analytical error, the variability in the source water concentration and the uncertainty in the fresh water estimates. The oceanic uptake of atmospheric CO_2 by Fransson et al. (2001) was determined by the difference in the export production computed from the nutrient deficit and the observed deficit of dissolved inorganic carbon. The uncertainty for this calculation procedure was estimated.

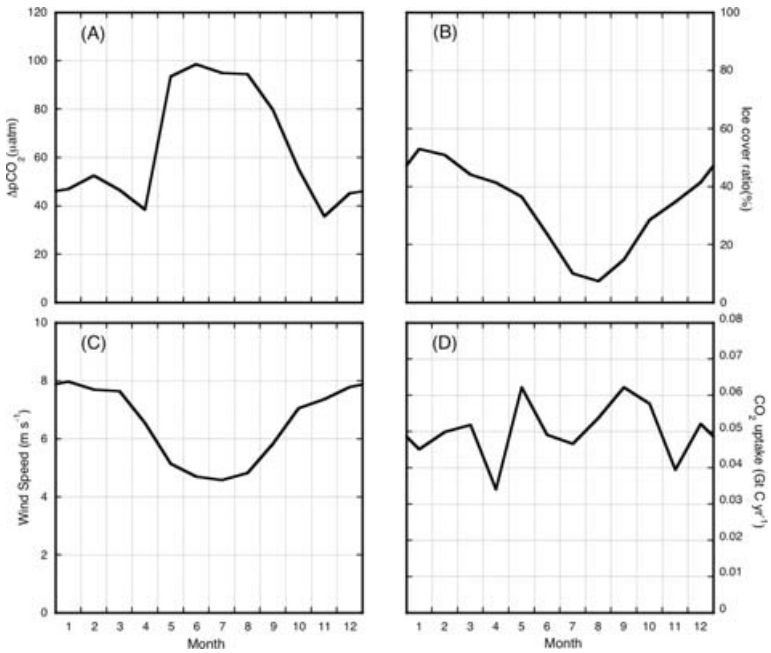

Fig. 7. Seasonal variations of ΔpCO_2 (A), the sea ice cover (B), the wind speed (C) and the CO_2 uptake (D) in the Greenland Sea and the Barents Sea (70°–80°N, 20°W–40°E).

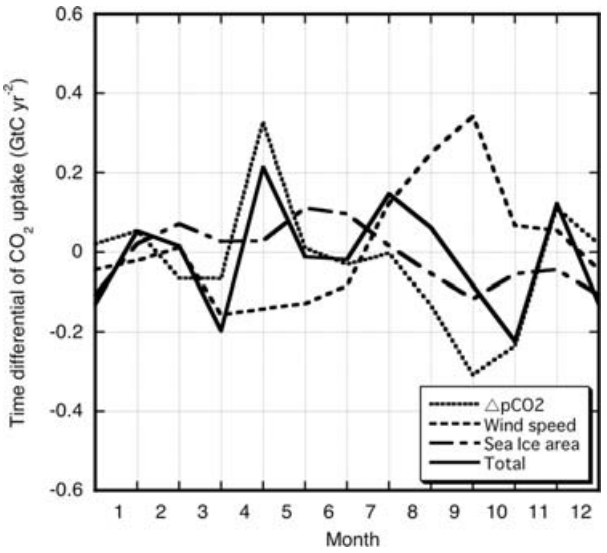

Fig. 8. Respective contributions of ΔpCO_2, the wind speed and the sea ice area to the seasonal variation of the oceanic CO_2 uptake in the Greenland Sea and the Barents Sea (*cf*. text). The positive and negative values mean the acceleration and suppression of the CO_2 uptake, respectively.

velocity and the ΔpCO_2. The differential of $F_{a.f.}(t)$ with respect to time can be written as

$$\frac{\delta F_{a.f.}}{\delta t} = \frac{\delta \overline{E(t)}}{\delta t} \cdot \Delta \overline{pCO_2(t)} \cdot S(t) \cdot + \overline{E(t)} \cdot \frac{\delta \Delta \overline{pCO_2(t)}}{\delta t} \cdot S(t) + \overline{E(t)} \cdot \Delta \overline{pCO_2(t)} \cdot \frac{\delta S(t)}{\delta t}, \quad (7)$$

where the first, second and third terms on the right-hand side of eq. (7) represent changes in the CO_2 uptake caused by temporal variations in the gas transfer coefficient, ΔpCO_2, and the sea area, respectively. The calculated values of the respective terms and their sum are given in Fig. 8. The decrease in the CO_2 uptake seen from March to April is caused by the reduction in both ΔpCO_2 and the wind speed. From April to May, these contributions tend to counteract each other, but the contribution from the ${pCO_2}^{sea}$ decrease becomes so large that the CO_2 uptake increases. For the period of August to October, the wind speed is a major factor for controlling the air–sea CO_2 flux. In November and December, the air–sea CO_2 flux increases, mainly due to rapid changes in ΔpCO_2. The seasonally varying sea ice area contributes to the decrease in the CO_2 uptake from September to November to a certain extent, but, compared with the wind speed and ΔpCO_2, it has a minor effect on the variations in the CO_2 uptake.

3.5. Interannual variability of the CO_2 flux in the Greenland Sea and the Barents Sea

We examined the interannual variability of the air–sea CO_2 flux in the same way as Olsen et al. (2003) did. We assumed that the only intercept values given in Table 2 for the empirical ${pCO_2}^{sea}$-SST relationships varied with the atmospheric CO_2 increase rate ($1.5\ \mu$atm yr^{-1}) over the period from 1992 to 2001. This assumption means that the ΔpCO_2 was not affected by the uptake of anthropogenic CO_2. Figure 9 shows the monthly and 1-year running mean anomalies of the ΔpCO_2, sea ice area, wind speed, CO_2 uptake, and the monthly and 1-year running means of the North Atlantic Oscillation Index (NAOI) during the same period. By comparing these anomalies with the average values of the CO_2 uptake and its relevant factors, i.e. the wind speed, ΔpCO_2 and sea ice area, we estimated the contributions of the anomalies of the respective factors to the CO_2 uptake to be 13, 4 and 15%, respectively. Considering the anomalies of the wind speed, SST and sea ice area, the interannual variability of the CO_2 uptake amounts was found to be 18% of its average value. Contrary to the equatorial Pacific, where large interannual variations in the air–sea CO_2 flux occur due to changes in the ΔpCO_2 distribution (Feely et al., 2002), the Greenland Sea and the Barents Seas are the oceans in which ΔpCO_2 is a minor factor in determining the interannual variability. Olsen et al. (2003) reported that the interannual variability of the CO_2 uptake for the entire North Atlantic Ocean in the winter season between 1981 and 2001 was about 7%. They also reported that changes in the wind speed and ${fCO_2}^{air}$ accounted for most of its interannual variations. Their finding that the wind speed is crucial for the interannual variations of the air–sea CO_2 flux is in agreement with our results.

The NAOI is an index derived from the north–south distribution of the sea level pressure over the North Atlantic Ocean. Therefore, the NAOI is closely related to the wind speed over the northern North Atlantic. The anomaly of the CO_2 uptake varies similarly with those of the wind speed and the NAOI. The anomalies of ΔpCO_2 and the sea ice area are negatively correlated with the NAOI. In the North Atlantic sector, the climate variability on a time scale of months to decades is dominated by the North Atlantic Oscillation (Wallace and Gutzler, 1981). Therefore, both the decadal change in CO_2 uptake and the interanuual variation could occur in the Greenland Sea and the Barents Sea.

Overland and Wang (2005) reported that the ice area has decreased by about 20% over the past two and a half decades, primarily in the western Arctic Ocean, and a decrease in sea ice has occurred in the last decade, as shown in Fig. 9 in their paper. Jones et al. (2001) reported an SST increase of 0.18 °C per decade in the Northern Hemisphere over the same period. The wind speed also seemed to decrease slightly, but not significantly, when an rms deviation of ± 3.0 m s^{-1} is taken into account (Smith et al., 2001). If these long-term trends are added to eq. (4), the CO_2 uptake is consequently expected to increase at a rate of 8×10^{-4} GtC yr^{-2}, which is mostly caused by the decrease in the sea ice area. Skjelvan et al. (1999) also suggested an increasing trend in the CO_2 uptake of about 9×10^{-4} GtC yr^{-2} in the Greenland Sea. These results indicate that more anthropogenic CO_2 will possibly be stored in the Greenland Sea and the Barents Sea due to a decrease in sea ice area in the near

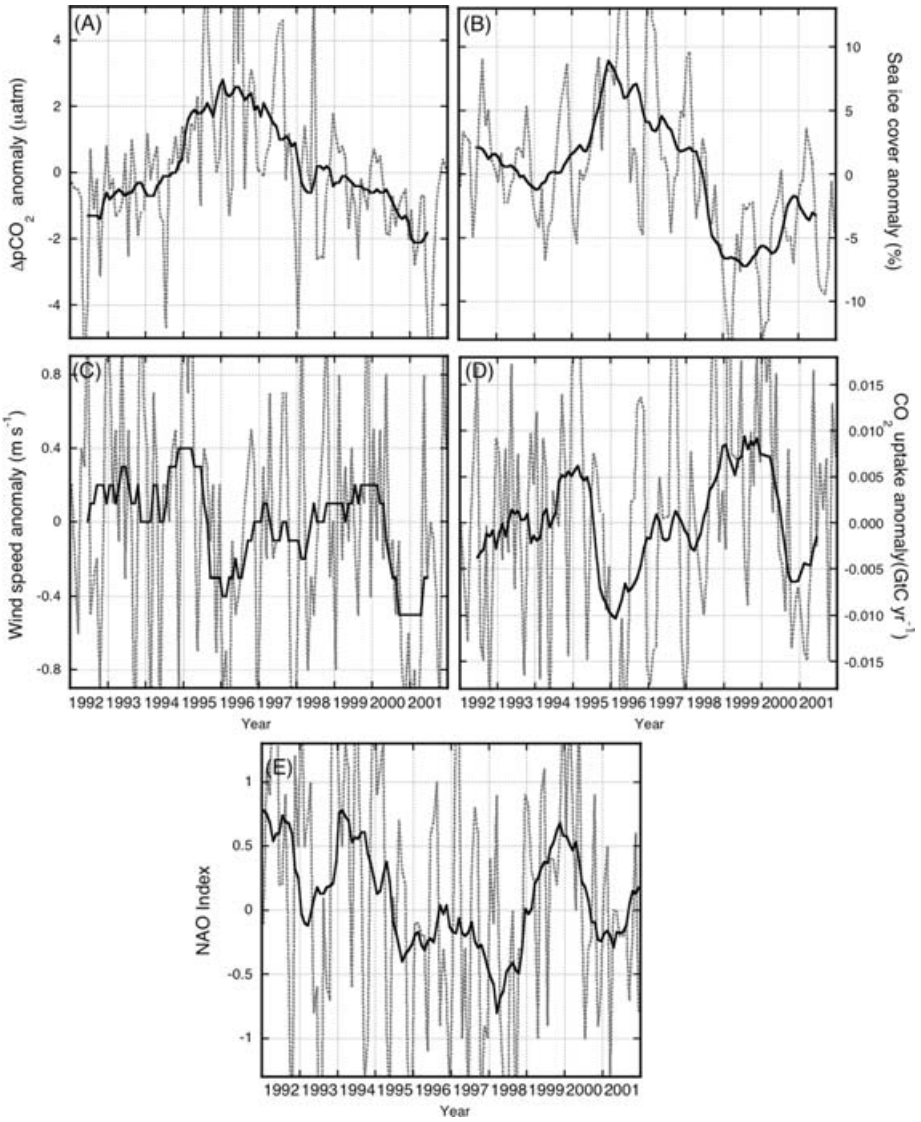

Fig. 9. Anomalies of ΔpCO_2 (A), the ice cover (B), the wind speed (C) and the CO_2 uptake (D) in the Greenland Sea and the Barents Sea, and those of the NAOI (E). The dashed lines represent the anomalies of the monthly means, and the solid lines show their 1-year running means.

future. However, the oceanic dynamics and biological activities in the near future may be different from the present conditions. Therefore, extended observations and analyses are needed to forecast the variation of air–sea CO_2 flux in the Greenland Sea and the Barents Sea.

4. Summary

Measurements of pCO_2^{sea} were made in the Greenland Sea and the Barents Sea from 1992 through 2001 by using a discrete sampling of the air equilibrated with surface seawater. The measured values of pCO_2^{sea} ranged between 200 and 350 μatm, which are generally lower than pCO_2^{air}, suggesting an effective transport of CO_2 from the atmosphere into intermediate/deep waters ventilated in these seas. The pCO_2^{sea} values showed a positive correlation with SST each month except for May and June, when a negative pCO_2^{sea}-SST relationship was found in the western Greenland Sea due to CO_2 drawdown by biological activities. Our pCO_2^{sea} data suggest a long-term increase, as do the data of Olsen et al. (2003) and Omar et al. (2003) for the North Atlantic Ocean and the Barents Sea, respectively.

By assuming that pCO_2^{sea} has increased at the same rate (1.5 μatm yr^{-1}) as pCO_2^{air}, we derived a set of seasonally varying pCO_2^{sea}-SST relationships for the Greenland Sea and the Barents Sea to estimate the pCO_2^{sea} values for the areas where no observation was conducted. In 1995, the values of pCO_2^{sea} calculated using those relationships and the SST data were found to be low in the northwestern Greenland Sea in July and August

(<220 μatm) and relatively high (>340 μatm) for warm water originating from the Norwegian Atlantic Current in April.

The air–sea CO_2 fluxes in 1995 were calculated using the gas transfer coefficient, wind speed and ΔpCO_2 derived from the $pCO_2{}^{sea}$-SST relationships, SST and $pCO_2{}^{air}$ at Ny-Ålesund. The air–sea CO_2 fluxes for the Greenland Sea ranged between 37 ± 14 gC m^{-2} yr^{-1} in summer and 72 ± 25 gC m^{-2} yr^{-1} in winter, showing an annual average of 52 ± 20 gC m^{-2} yr^{-1}. On the other hand, the CO_2 fluxes for the Barents Sea were found to be 28 ± 13 gC m^{-2} yr^{-1} in spring and 63 ± 22 gC m^{-2} yr^{-1} in winter, with an annual average of 46 ± 18 gC m^{-2} yr^{-1}. The total CO_2 uptake in the Greenland Sea and the Barents Sea (70°–80°N, 20°W–40°E) was within the range of 0.034 ± 0.014 in summer to 0.062 ± 0.024 GtC yr^{-1} in winter with an annual mean of 0.050 ± 0.020 GtC yr^{-1}.

We also examined the sensitivity of seasonal/interannual variations of the oceanic CO_2 uptake to the gas transfer coefficient as a function of wind speed, ΔpCO_2 and the sea ice area. The results showed that both the wind field and ΔpCO_2 were particularly important for the seasonal variation in the CO_2 uptake. The interannual variability of the 1-year running mean was estimated to be $\pm$ 18% of the oceanic CO_2 uptake of 0.050 GtC yr^{-1}. The wind speed anomaly showed a positive correlation with the NAOI, while the anomalies of ΔpCO_2 and the sea ice area were negatively correlated with the index. The CO_2 uptake anomaly showed temporal variations similar to the NAOI. It was also found that the interannual variability of the CO_2 uptake was noticeably influenced by the wind speed (13%, relative to the mean annual CO_2 uptake) and the sea ice area (15%), while the contribution of ΔpCO_2 (4%) was minor.

5. Acknowledgments

We would like to sincerely thank Drs. Leif G. Anderson and Taro Takahashi for providing their oceanic CO_2 data. We also appreciate the staff of the Norwegian Polar Institute and the crew of the R/V LANCE for their continuous cooperation with our measurements.

References

Aagaard, K., Swift, J. H. and Carmack, E. C. 1985. Thermohaline circulation in the Arctic Mediterranean seas. *J. Geophys. Res.* **90**, 4833–4846.

Anderson, L. G. 1995. Chemical oceanography of the Arctic and its shelf seas. In: *Arctic Oceanography: Marginal Ice Zones and Continental Sand Estuarine Studies* (eds W. O. Smith, Jr. and J. M. Grebmeier). American Geophysical Union, Washington, DC, pp. 183–202.

Anderson, L. G., Drange, H., Chierici, M., Fransson, A., Johannessen, T. and co-authors. 2000. Annual carbon fluxes in the upper Greenland Sea based on measurements and a box-model approach. *Tellus* **52B**, 1013–1024.

Broecker, W. S. and Peng, T. H. 1982. *Tracer in the Sea*, 690 pp. Eldigio Press, Palisades, New York.

Cosca, C. E., Feely, R. A., Boutin, J., Etcheto, J., McPhaden, M. J. and co-authors 2003. Seasonal and interannual CO_2 flux for the central and eastern equatorial Pacific Ocean as determined from fCO_2-SST relationships. *J. Geophys. Res.* **108(C8)**, 3278, doi:10.1029/2000JC000677.

Dandonneau, Y. 1995. Sea-surface partial pressure of carbon dioxide in the eastern equatorial Pacific (August 1991 to October 1992): a multivariate analysis of physical and biological factors. *Deep-Sea Res. II* **42**, 349–364.

Feely, R. A., Boutin, J., Cosca, C. E., Dandonneau, Y., Etcheto, J. and co-authors 2002. Seasonal and interannual variability of CO_2 in the equatorial Pacific. *Deep-Sea Res. II* **49**, 2443–2470.

Francey, R. J., Tans, P. P., Allison, C. E., Enting, I. G., White, J. W. C. and co-author 1995. Changes in oceanic and terrestrial carbon uptake since 1982. *Nature* **373**, 326–330.

Fransson, A., Chierici, M., Anderson, L. G., Bussman, I., Jones, E. P. and co-author 2001. The importance of shelf processes for the modification of chemical constituents in the waters of the eastern Arctic Ocean. *Shelf Res.* **21**, 225–242.

Furevik, T. 2001. Annual and interannual variability of Atlantic water temperatures in the Norwegian and Barents Seas: 1980–1996. *Deep-Sea Res. I* **48**, 383–404.

Gruber, N., Keeling, C. D. and Bates, N. R. 2002. Interannual variability in the North Atlantic Ocean carbon sink. *Science* **298**, 2374–2378.

Hood, E. M., Merlivat, L. and Johannessen, T. 1999. Variations of fCO_2 and air-sea flux of CO_2 in the Greenland Sea gyre using high-frequency time series data from CARIOCA drift buoys. *J. Geophys. Res.* **104(C9)**, 20 571–20 583.

Inoue, H. Y., Matsueda, H., Ishii, M., Fushimi, K., Hirota, M., Asanuma, I. and Takasugi, Y. 1995. Long-term trend of the partial pressure of carbon dioxide (pCO_2) in surface waters of the western North Pacific 1984–1993. *Tellus* **47B**, 391–413.

Inoue, H. Y. and Ishii, M. 2005. Variations and trend of CO_2 in the surface seawater in the Southern Ocean south of Australia between 1969 and 2002. *Tellus* **57B**, 58–69.

Jones, P. D., Osborn, T. J., Briffa, K. R., Folland, C. K., Horton, E. B. and co-authors 2001. Adjusting for sampling density in grid box land and ocean surface temperature time series. *J. Geophys. Res.* **106**, 3371–3380.

Kalnay, E., Kanamitsu, M., Kistler, R., Collins, W., Deaven, D. and co-authors 1996. The NCEP/NCAR 40-Year Reanalysis Project. *Bull. of Am. Meteorol. Soc.* **77**, 437–472.

Kaltin, S., Anderson, L. G., Olsson, K., Fransson, A. and Chierici, M. 2002. Uptake of atmospheric carbon dioxide in the Barents Sea. *J. Marine Systems* **38**, 31–45.

Keeling, R. F. and Shertz, S. R. 1992. Seasonal and interannual variations in atmospheric oxygen and implications for the global carbon cycle. *Nature* **358**, 723–727.

Keeling, C. D., Whorf, T. P., Wahlen, M. and van der Plicht, J. 1995. Interannual extremes in the rate of rise of atmospheric carbon dioxide since 1980. *Nature* **375**, 666–670.

Keeling, C. D., Brix, H. and Gruber, N. 2004. Seasonal and long-term dynamics of the upper ocean carbon cycle at Station ALOHA near Hawaii. *Global Bogeochem. Cycles* **18**, GB4006, doi:10.1029/2004GB002227.

Lefèvre, N., Watson, A. J., Olsen, A. and Johannessen, T. 2004. A decrease in the sink for atmospheric CO_2 in the North Atlantic. *Geophys. Res. Lett.* **31**, L07306 doi:10.1029/2003GL018957.

Le Quéré, C., Aumont, O., Bopp, L., Bousquet, P., Ciais, P. and co-authors. 2003. Two decades of ocean CO_2 sink and variability. *Tellus* **55B**, 649–656.

Midorikawa, T., Nemoto, K., Kamiya, H., Ishii, M. and Inoue, H. Y. 2005. Persistently strong oceanic CO_2 sink in the western subtropical North Pacific. *Geophys. Res. Lett.* **32**, L05612, doi:10,1029/2004GL021952.

Morimoto, S., Aoki, S. and Yamanouchi, T. 2001. Temporal variations of atmospheric CO_2 concentration and carbon isotope ratio in Ny-Ålesund, Svalbard, "Environmental Research in the Arctic 2000". *Mem. Natl. Inst. Polar Res. Spec. Issue* **54**, 71–80.

Nakazawa, T., Morimoto, S., Aoki, S. and Tanaka, M. 1997. Temporal and spatial variations of the carbon isotopic ratio of atmospheric carbon dioxide in the western Pacific region. *J. Geophys. Res.* **102**, 1271–1285.

Noji, T. T., Miller, L. A., Skjelvan, I., Falck, E., Børsheim, K. Y. and co-authors. 2000. Constrains on carbon drawdown and export in the Greenland sea. In: *The Northern North Atlantic: A Changing Environment* (eds. P. Schäfer, W. Ritzrau, M. Schlüter and J. Thiede). Springer, Berlin. pp. 39–52.

Olsen, A., Bellerby, R. G. J., Johannessen, T., Omar, A. and Skjelvan, I. 2003. Interannual variability in the wintertime air-sea flux of carbon dioxide in the northern North Atlantic, 1981–2001. *Deep-Sea Res. I* **50**, 1323–1338.

Omar, A., Johannessen, T., Kaltin, S. and Olsen, A. 2003. Anthropogenic increase of oceanic pCO_2 in the Barents Sea surface water. *J. Geophys. Res.* **108**(**C12**), 3388, doi:10.1029/2002JC001628.

Overland, J. E. and Wang, M. 2005. The Arctic climate paradox: the recent decrease of the Arctic oscillation. *Geophys. Res. Lett.* **32**, L06701, doi:10.1029/2004GL021752.

Prentice, I. C., Farquhar, G. D., Fasham, N. J. R., Goulden, M. L., Heimann, M. and co-authors. 2001. The carbon cycle and atmospheric CO_2. In: *Climate Change: The Scientific Basis, the Contribution of WG1 of the IPCC to the IPCC Third Assessment Report (TAR)* (eds. J. T. Houghton and D. Yihui). Cambridge University Press, Cambridge, UK, pp. 183–237.

Rayner, P. J., Enting, I. G., Francey, R. J. and Langenfelds, R. L. 1999. Reconstructing the recent carbon cycle from atmospheric CO_2, $\delta^{13}C$ and O_2/N_2 observations. *Tellus* **51B**, 213–232.

Schlosser, P., Bönisch, G., Kromer, B. and Münnich, K. O. 1990. Ventilation rates in the Nansen Basin of the Arctic Ocean derived from a multitracer approach. *J. Geophys. Res.* **95**, 3265–3272.

Skjelvan, I., Johannessen, T. and Miller, L. A. 1999. Interannual variability of CO_2 in the Greenland and Norwegian Seas. *Tellus* **51B**, 477–489.

Smith, S. R., Legler, D. M. and Verzone, K. V. 2001. Quantifying uncertainties in NCEP reanalysis using high-quality research vessel observations. *J. Climate* **14**, 4062–4072.

Takahashi, T., Olafsson, J., Godard, J. G., Chipman, D. W. and Sutherland, S. C. 1993. Seasonal variation of CO_2 and nutrient in the high-latitude surface oceans: a comparative study. *Global Biogeochem. Cycles* **7**(**4**), 843–878.

Takahashi, T., Stewart, C. S., Sweeney, C., Poisson, A., Metzl, N. and co-authors. 2002. Global sea-air CO_2 flux based on climatological surface ocean pCO_2, and seasonal biological and temperature effects. *Deep-Sea Res. II* **49**, 1601–1622.

Tanaka, M., Nakazawa, T. and Aoki, S. 1987. Time and space variations of tropospheric carbon dioxide over Japan. *Tellus* **39B**, 3–12.

Tans, P. P., Fung, I. Y. and Takahashi, T. 1990. Observational constraints on the global atmospheric CO_2 budget. *Science* **247**, 1431–1438.

Wallace, J. M. and Gutzler D. S. 1981. Teleconnections in the geopotential height field during the Northern Hemisphere winter. *Mon. Wea. Rev.* **109**, 784–812.

Wanninkhof, R. 1992. Relationship between wind speed and gas exchange. *J. Geophys. Res.* **97**, 7373–7382.

Wanninkhof, R. and McGills, W. R. 1999. A cubic relationship between air-sea CO_2 exchange and wind speed. *Geophys. Res. Lett.* **26**, 1889–1993.

Wanninkhof, R., Feely, R. A., Chen, H., Cosca, C. E. and Murphy, P. P. 1996. Surface water fCO_2 in the eastern equatorial Pacific during the 1992–1993 El Niño. *J. Geophys. Res.* **101**, 16 333–16 343.

Watai, T., Kikuchi, M. and Nakazawa, T. 1998. Temporal variations of surface oceanic and atmospheric CO_2 fugacity and total dissolved inorganic carbon in the northwestern North Pacific. *J. Oceanogr.* **54**, 323–336.

Weiss, R. F. 1974. Carbon dioxide in water and seawater: the solubility of a non-ideal gas. *Mar. Chem.* **2**, 203–215.

Weiss, R. F., Van Woy, F. A. and Salameh, P. K. 1992. Surface water and atmospheric carbon dioxide and nitrous oxide observations by shipboard automated gas chromatography: results from expeditions between 1977 and 1990. Scripps Institute of Oceanography. Carbon Dioxide Information Analysis Center Oak Ridge National Laboratory. NDP-044.